

Adaptive compressive tomography with no *a priori* information

D. Ahn, Y. S. Teo,* and H. Jeong

Department of Physics and Astronomy, Seoul National University, 08826 Seoul, South Korea

F. Bouchard, F. Hufnagel, and E. Karimi

Physics Department, University of Ottawa, 25 Templeton Street, Ottawa, Ontario, K1N 6N5 Canada

D. Koutný, J. Řeháček, and Z. Hradil

Department of Optics, Palacký University, 17. listopadu 12, 77146 Olomouc, Czech Republic

G. Leuchs and L. L. Sánchez-Soto

Max-Planck-Institut für die Physik des Lichts, Staudtstraße 2, 91058 Erlangen, Germany

Quantum state tomography is both a crucial component in the field of quantum information and computation, and a formidable task that requires an incogitable number of measurement configurations as the system dimension grows. We propose and experimentally carry out an intuitive adaptive compressive tomography scheme, inspired by the traditional compressed-sensing protocol in signal recovery, that tremendously reduces the number of configurations needed to uniquely reconstruct any given quantum state without any additional *a priori* assumption whatsoever (such as rank information, purity, etc) about the state, apart from its dimension.

Introduction.—The characterization of an unknown (true) quantum state $\rho_t \geq 0$ of Hilbert-space dimension d is a subject of immense study in quantum information [1–3]. To fully reconstruct an *arbitrary* ρ_t , one may perform a set of measurements that is enough to characterize all $d^2 - 1$ independent parameters that define ρ_t . Unfortunately, the number of such measurements generally grows polynomially with d , or exponentially with the number of subsystems that determine the quantum-source complexity. This poses a technical limitation on how far conventional quantum tomography can go in practical experiments [4, 5].

If we know *a priori* that $\text{rank}\{\rho_t = \rho_r\} \leq r$ is extremely small, $r \ll d$, then the concept of compressed sensing (CS), whose foundation was first mathematically laid in the context of imaging [6–8], facilitates the search for a unique estimator by measuring much fewer configurations [9–12]. We say that the corresponding data are *informationally complete (IC)* for ρ_r . The state-of-the-art CS measurements to be performed given such a prior information have been constructed in [13].

The standard CS procedure, nevertheless, has two important issues that need to be addressed. Firstly, an *a priori* knowledge about r is necessary to establish a preliminary order-of-magnitude estimate for the number of configurations needed to fully characterize ρ_r of rank no larger than r . Accuracy of the final estimator is hence highly dependent on the validity of this *a priori* guess. Secondly, one has no means of verifying whether the measurement data at hand are truly IC for ρ_r in the standard scheme. Typically, accuracy surveys with target states are employed [10–12] and the value of such a survey relies on the precision of these target states. Therefore, the decision of *a priori* rank information and presumed choices of target states are ultimately debatable in the presence of experimental errors, rendering the reliability of any related tomography scheme questionable.

In this Letter, we establish a new adaptive tomography paradigm that completely removes the need for any sort of *a priori* information about ρ_r (except for its dimension d). Our proposed *adaptive compressive tomography (ACT)* also includes an efficient recipe to determine informational completeness of the collected data. No target states are ever required to validate the resulting state estimator. The convex boundary of the quantum state space and the positivity constraint plays the principal role in checking whether the accumulated data are IC and adaptively choosing measurements efficiently to uniquely reconstruct ρ_r , the two of which completely define the purpose of ACT.

To demonstrate ACT, we perform an experiment with the orbital angular momentum (OAM) of single photons and apply ACT to states of various ranks engineered in these degrees of freedom. Both experimental and simulated results show that ACT requires a smaller number of measurements to reconstruct rank-deficient quantum states as compared to conventional CS tomography with known types of CS measurements.

The quantum state space and ACT.—In the absence of statistical fluctuations, we measure a randomly chosen computational basis $\{|0\rangle, |1\rangle, \dots, |d-1\rangle\}$ on ρ_r of Hilbert-space dimension d . The corresponding Born probabilities $p_j = \langle j | \rho_r | j \rangle$ ($0 \leq j \leq d-1$) specify only the diagonal elements of ρ_r , and there is in principle a *data convex set* $\mathcal{C} = \{\rho | \rho \leftrightarrow p_j \forall j\}$ comprising infinitely many estimators $\hat{\rho}$ that are consistent with p_j . Evidently, $\rho_r \in \mathcal{C}$, and so the only fundamental objective of ACT is to shrink \mathcal{C} to a single point with only $k_{\text{IC}} \ll d+1$ IC measurement bases for $r \ll d$. For noiseless situations, this point must be ρ_r .

To gain insights into how quantum positivity constraint plays a major role in shrinking \mathcal{C} , we argue in Appendix A that if one methodically measures $k_0 = \lceil (r^2 - r)/(d-1) \rceil + 1$ orthonormal bases, one of which being the eigenbasis \mathcal{B}_{ρ_r} of ρ_r , then $\hat{\rho} = \rho_r$ is the *unique positive estimator* consistent with all measured probabilities. For $r \ll d$, the regime of our inter-

* ys_teo@snu.ac.kr

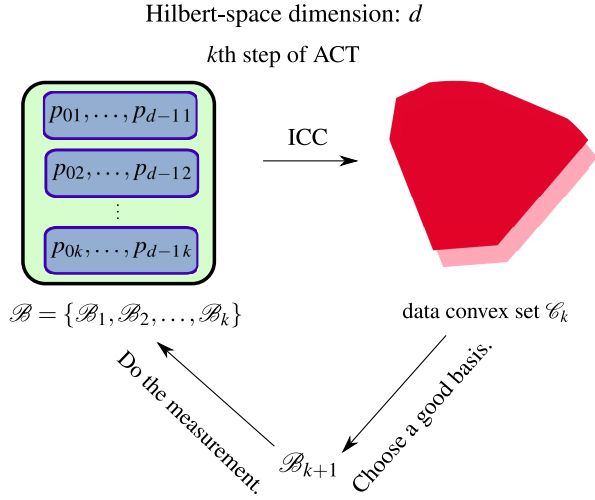


FIG. 1. Schematic diagram of a particular adaptive step in ACT tomography. In a clockwise flow, ACT first performs ICC to check whether data (blue) collected from measuring \mathcal{B} are IC or not. If not, it proceeds to choose a good basis to measure in the next step.

est, $k_0 = 2$. It is however clear that $k_{\text{IC}} > 2$ in real-world settings where ρ_r is completely unknown (apart from its dimension d), so the famous no-go answer to Pauli’s phase-retrieval problem [14, 15] still stands. Regardless the positivity constraint can still ensure an efficient compression of the IC tomography procedure solely by data analysis.

The goal of ACT is to uniquely reconstruct any given unknown ρ_r through adaptively measuring one orthonormal basis at a time according to collected data, as sketched in Fig. 1. In the k th step of the adaptive scheme, ACT performs two main procedures. (I) First, ACT checks whether the probabilities $p_{j'k'} = \text{tr}\{\rho_r \Pi_{j'k'}\}$ obtained from outcomes $\Pi_{j'k'} > 0$ ($\Pi_{j'k'} \Pi_{j''k''} = \delta_{j',j''} \delta_{k',k''}$) of all the measured orthonormal bases $\mathcal{B} = \{\mathcal{B}_1, \mathcal{B}_2, \dots, \mathcal{B}_k\} = \{\Pi_{01}, \dots, \Pi_{d-1,1}, \dots, \Pi_{0k}, \dots, \Pi_{d-1,k}\}$ so far are IC. Since the *accumulated* data define a data convex set \mathcal{C}_k of size s_k that contains all quantum states ρ consistent with $p_{j'k'}$, this procedure is tantamount to finding out whether s_k is zero or not. If $s_{k=k_{\text{IC}}} = 0$, then the estimator $\hat{\rho}_{k=k_{\text{IC}}} \geq 0$ consistent with the IC data is unique by definition, and equal to ρ_r when statistical fluctuation is absent. (II) If $s_k \neq 0$, the accumulated data collected are not IC and ACT shall choose the next basis by analyzing \mathcal{C}_k . Beginning with $k = 1$, a “good” adaptive bases sequence should lead to a quick convergence of $\mathcal{C} \rightarrow \rho_r$ as ACT progresses.

(I) *Informational completeness certification (ICC)*.—To certify whether all collected data are IC or not in the k th adaptive step, it suffices to note that since \mathcal{C}_k is convex, maximizing and minimizing the linear function $f_Z(\rho) = \text{tr}\{\rho Z\}$ for some operator Z over $\rho \in \mathcal{C}_k$ respectively give unique solutions ρ_{max} and ρ_{min} to the corresponding maximum $f_{\text{max},k}$ and minimum $f_{\text{min},k}$. Without loss of generality, Z is taken to be a random full-rank state. We may define the quantity $s_{\text{CVX},k} = (f_{\text{max},k} - f_{\text{min},k}) / (f_{\text{max},1} - f_{\text{min},1})$ that is a *size monotone* (see Appendix B) for \mathcal{C}_k in the sense that $s_k < s_{k-1}$ if

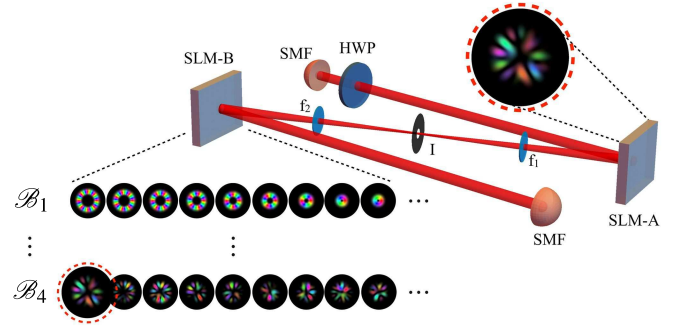


FIG. 2. Schematic of the OAM-based experimental setup. A 16-dimensional OAM state is generated at SLM-A using a holographic technique that allows the tailoring of the intensity and phase profile of the incoming beam. The modulated first-order of diffraction is filtered out using an iris (I) and a pair of lenses (f_1 and f_2). A similar holographic technique is used at the second SLM-B to measure the state in a given basis. The first measurement basis, \mathcal{B}_1 , is given by the OAM computational basis. In the case of the rank 1 state shown on SLM-A, the corresponding eigenbasis is achieved after the fourth iteration.

$s_{\text{CVX},k} < s_{\text{CVX},k-1}$ —it is a witness for the shrinkage of \mathcal{C}_k . As more linearly independent bases are measured, $s_{\text{CVX},k} \geq s_{\text{CVX},k+1}$, and $s_{\text{CVX},k_{\text{IC}}} = 0$ implies that $s_{k_{\text{IC}}} = 0$ and that all data collected are IC for a unique reconstruction of ρ_r . Therefore, at every adaptive step in ACT, we run:

ICC in the k th step

1. Maximize and minimize $f_Z(\rho) = \text{tr}\{\rho Z\}$ for a fixed, randomly-chosen full-rank state $Z \neq 1/d$ to obtain $f_{\text{max},k}$ and $f_{\text{min},k}$ subject to
 - $\rho \geq 0$, $\text{tr}\{\rho\} = 1$,
 - $\text{tr}\{\rho \Pi_{j'k'}\} = p_{j'k'}^{(\text{ML})}$ for $0 \leq j' \leq d-1$ and $1 \leq k' \leq k$.
2. Compute $0 \leq s_{\text{CVX},k} \leq 1$ and check if it is smaller than some threshold ε .
3. If $s_{\text{CVX},k} < \varepsilon$, terminate ACT. Continue otherwise.

The aforementioned strategy is, as a matter of fact, a semidefinite program (SDP) [16] that can be efficiently solved by a variety of numerical methods. We should clarify here that while determining whether a set of measurement bases \mathcal{B} possesses the conventional CS property for the entire class of rank- r states is an NP-hard problem [17], ascertaining whether \mathcal{B} gives a unique estimator for one unknown ρ_r with the measurement data is, on the other hand, only as computationally difficult as carrying out the semidefinite program in ICC with a worst-case polynomial complexity [16].

For experimental data $\sum_{j'} v_{j'k'} = 1$ ($1 \leq k' \leq k$) with statistical noise, \mathcal{C}_k is defined as the *maximum-likelihood (ML) convex set* in which all $\rho \in \mathcal{C}_k$ satisfy the physical constraints $p_{j'k'}^{(\text{ML})} = \text{tr}\{\rho \Pi_{j'k'}\}$ imposed by the ML principle for quan-

tum states $\left[p_{j'k'}^{(\text{ML})} \rightarrow p_{j'k'} \text{ for } N \rightarrow \infty \right]$ [2, 3, 18, 19]. All arguments for noiseless data hold exactly for the ML probabilities, so that the working principle of ICC is *perfectly robust against arbitrary noise* in the sense that $s_{\text{CVX},k_{\text{IC}}} = 0$ still implies $s_{k_{\text{IC}}} = 0$ for noisy data owing to the preserved convexity of the newly defined \mathcal{C}_k . Noise only affects the reconstruction accuracy of the final unique estimator relative to ρ_r , which is a different subject matter for discussion.

(II) *Adaptive selection of measurement bases.*—The optimal orthonormal basis to pick in the k th step and measure in the $(k+1)$ th step is the one that minimizes $s_{\text{CVX},k+1}$. Since ρ_r is unknown, we can treat some *a posteriori* estimator $\hat{\rho}_k$ from \mathcal{C}_k as a guess for ρ_r to generate simulated data during the minimization of $s_{\text{CVX},k+1}$ over all future basis choices. The complicated dependence of $s_{\text{CVX},k+1}$ on the future basis however makes its brute-force optimization computationally exhaustive for large d .

For a more tractable approach to adaptively measure good bases, we first note that $\mathcal{C}_{k < k_{\text{IC}}}$ *essentially* contains states with eigenbases that are distinct from $\{\mathcal{B}_1 \dots \mathcal{B}_k\}$ (see Appendix C). So even if we know nothing about ρ_r , if it is rank-deficient, then taking \mathcal{B}_{k+1} to be the diagonal basis of a rank-deficient $\hat{\rho}_k \in \mathcal{C}_k$ ensures a distinct measurement basis in each step that generates a reasonably fast converging sequence $\mathcal{B}_k \rightarrow \mathcal{B}_{\rho_r}$ as k increases since $\mathcal{C}_k \rightarrow \rho_r$ at the same time. There is more than one approach to pick eigenbases of rank-deficient states from \mathcal{C}_k , and as an example we shall consider the minimization of von Neumann entropy function $S(\rho) = -\text{tr}\{\rho \log \rho\}$. A superfast algorithm suitable for minimizing S over \mathcal{C}_k exists [19, 20]. Incidentally, it was reported in [21, 22] that entropy minimization also offers high compressive efficiencies in both sparse-signal and low-rank matrix recovery.

Complete ACT protocol.—All aforementioned arguments can accommodate real experimental situations, where the relative frequency data do not typically correspond to physical quantum states for $k > 1$. The data convex sets contain states that are now consistent with the corresponding physical ML probabilities derived from data, which are statistically consistent with the true probabilities. The final unique estimator $\hat{\rho}_{k_{\text{IC}}}$ would then incur a statistical bias from ρ_r that drops as N increases. For many-body quantum sources, the bases generated by ACT are entangled. In practice, product bases are typically much more practical to implement for such sources. While verifying if a rank-deficient $\hat{\rho}_k \in \mathcal{C}_k$ can possess a product eigenbasis is computationally difficult, ACT can still be adjusted to feasibly generate near-optimal product bases (pACT) by defining \mathcal{B}_{k+1} to be the product basis that is nearest to the eigenbasis of $\hat{\rho}_k$ with respect to some given norm using a nonlinear optimization routine. Both ACT and pACT for any experimental setting are summarized:

ACT/pACT

Beginning with $k = 1$ and a random computational basis \mathcal{B}_1 :

1. Measure \mathcal{B}_k and collect the relative frequency data $\sum_{j'=0}^{d-1} v_{j'k} = 1$.
 2. From $\{v_{0k}, \dots, v_{d-1k}\}_{k'=1}^k$, obtain kd physical ML probabilities.
 3. Perform ICC with the ML probabilities and compute $s_{\text{CVX},k}$:
 - **If** $s_{\text{CVX},k} < \varepsilon$, terminate ACT and take $\rho_{\text{max}} \approx \rho_{\text{min}}$ as the estimator and report $s_{\text{CVX},k}$.
 - **Else** Proceed.
 4. Choose a rank deficient $\hat{\rho}_k \in \mathcal{C}_k$ [for instance by minimizing the von Neumann entropy $S(\rho)$ in \mathcal{C}_k].
 5. Define \mathcal{B}_{k+1} to be the eigenbasis of $\hat{\rho}_k$ for ACT, or a basis close to it for pACT *via* some prechosen distance minimization technique.
 6. Set $k = k + 1$ and repeat.
-

Analysis and experiments.—We put both ACT and pACT tomography schemes to the experimental test by comparing their results with those from measuring random Pauli (RP) bases considered in [10–12], the Baldwin–Goyeneche (BG) bases in [13] that generalizes a known five-bases construction for $r = 1$ to an IC set of $k_{\text{IC}} = 4r + 1$ bases for rank- r quantum states, and the set of random orthonormal bases of $k_{\text{IC}} \approx \lceil 4r(d-r)/(d-1) \rceil$ studied in [23]. This exact scaling shall be used to benchmark the experimental $k_{\text{IC}}s$.

To demonstrate all three schemes (see Fig. 2), we experimentally emulate a 4-qubit ($d = 16$) quantum system and both entangled and product measurement bases using an OAM-based setup. In particular, we consider the Laguerre-Gauss (LG) modes with azimuthal and radial mode indices ℓ and $p = 0$, respectively. Hence, OAM states correspond to a sub-space of the LG modes and are characterized by a helical wavefront given by $e^{i\ell\phi}$, where ℓ is the azimuthal index that corresponds to the OAM value, and ϕ is the azimuthal coordinate. The appropriate phase and intensity patterns are realized using a holographic technique called *intensity masking*, which is readily achieved by a programmable spatial light modulator (SLM) [24]. By doing so, we can prepare *any* many-body state and measurement basis. The generated photons are detected using the projective technique of *intensity-flattening* [25], where any arbitrary spatial mode can be measured using an SLM followed by a single mode fiber (SMF).

A heralded single photon source is achieved by pumping a 3 mm β -barium borate type I nonlinear crystal with a quasi-continuous wave laser at a wavelength of 355 nm, producing photon pairs at 710 nm via spontaneous parametric down-conversion. A coincidence rate of 40 kHz, within a coinci-

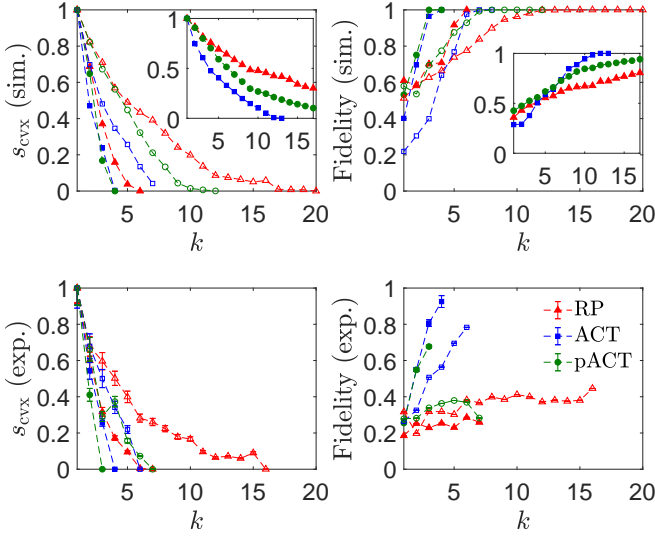


FIG. 3. Plots of simulation (noiseless) and experimental values of s_{cvx} and $\hat{\rho}_k$ fidelity against the measured basis number k for $d = 16$, where $\hat{\rho}_k := \rho_{\min}$ for the RP scheme. Estimated experimental error bars reflect the propagated Poissonian-source standard deviations. All plot markers are averaged over five ρ_r s. The filled markers represent results for rank-1 ρ_r s whereas the unfilled ones represent those for rank-3 ρ_r s. The insets showcase simulation performances of rank-6 states as a demonstration of high-rank ($r \approx D/2$) compressive tomography, with $1 \leq k \leq (D+1) = 17$ restricted to the minimal bases number for arbitrary-state tomography. The lower experimental fidelities for RP and pACT are due to a technical bias of the OAM setup for finite N , where bases close to the eigenbasis of ρ_r tend to give estimated Born probabilities that are relatively more accurate than those that are not. So for OAM sources, ACT is the most favorable option, as both pACT and RP correspond to measurement bases that are never close to the eigenbasis of ρ_r . Even with noisy data, ICC can still validate whether the resulting ML probabilities obtained from data are IC (left panels), which is the point of ACT.

dence time window of 5 ns, is measured after filtering the photons to the fundamental Gaussian modes using SMF. Subsequent to the generation and detection of the photonic states, explained above, coincidence measurements are recorded using single photon detectors and a coincidence logic.

All results are summarized in Figs. 3 and 4, and the messages conveyed are succinctly stated here: For noiseless simulated data, in terms of *average* k_{IC} over uniformly (Hilbert-Schmidt) distributed rank- r true states, ACT is the most efficient, since it guides the measurement basis to the eigenbasis of ρ_r . The more many-body-suited pACT that adaptively generates product bases requires a larger k_{IC} to yield IC data, but the average performance margin with ACT is narrow for low- r states and is on par with the scaling of entangled Goyeneche-type bases ($k_{\text{IC}} = 4r + 1$) for larger r . RP turns out to be least efficient amongst all tested schemes. Even in the presence of real data noise, both ACT and pACT remain the more favorable candidates for tomography on general complex systems.

Concluding remarks.—The feasible concept of adaptive compressive tomography developed here provides a powerful method to reconstruct any unknown rank-deficient quantum

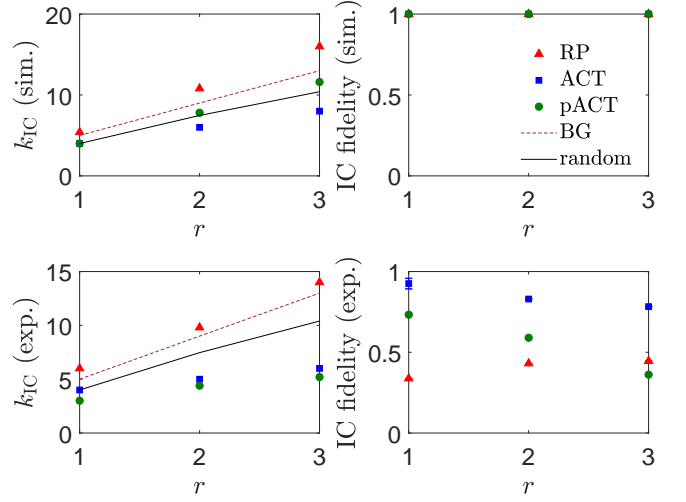


FIG. 4. Plots of simulation (noiseless) and experimental values of k_{IC} and the $\hat{\rho}_{k=k_{\text{IC}}}$ fidelity against the rank $1 \leq r \leq 3$ of ρ_r . All k_{IC} values ascertained using ICC are averaged over five ρ_r s per rank. Otherwise all specifications are the same as Fig. 3. Although for real data, positivity modifies the k_{IC} performances with ML, pACT achieves informational completeness much quicker than RP as far as local bases are concerned. A comparison with random IC orthonormal bases shows that ACT gives a much lower value owing to the additional assessment of and optimization over \mathcal{C} .

state with optimally chosen entangled or product orthonormal measurement bases, especially for quantum sources of complex degrees of freedom, which includes many-body systems. More importantly, the adaptive scheme requires no *a priori* knowledge or assumptions about the state or near-proximity target states because it can self-sufficiently validate whether the measured data are informationally complete or not using semidefinite programming, so that reliable compressive tomography can now be carried out in real experimental situations with noisy data. The superior compressive efficiencies of both entangled and product versions of our adaptive schemes are confirmed experimentally and demonstrated with respect to other established protocols.

We acknowledge financial support from the BK21 Plus Program (21A2013111123) funded by the Ministry of Education (MOE, Korea) and National Research Foundation of Korea (NRF), the NRF grant funded by the Korea government (MSIP) (Grant No. 2010-0018295), the Korea Institute of Science and Technology Institutional Program (Project No. 2E27800-18-P043), the European Union's Horizon 2020 Research and Innovation Programme under Grant Agreement No. 766970, Canada Research Chairs (CRC), the Spanish MINECO (Grant No. FIS2015-67963-P), the Grant Agency of the Czech Republic (Grant No. 18-04291S), and the IGA Project of the Palacký University (Grant No. IGA PrF 2018-003).

Appendix A: Uniqueness property induced by the state-space boundary

Suppose that the eigenbasis $\{|\lambda_j\rangle\}$ of a rank- r

$$\rho = \rho_r = \sum_{j=0}^{r-1} |\lambda_j\rangle p_j \langle \lambda_j| \quad (\text{A1})$$

is measured and the probabilities $\sum_{j=0}^{r-1} p_j = 1$ are collected, the estimator $\hat{\rho} = \rho_r$ is one solution that is consistent with the Born probabilities $\langle \lambda_j | \hat{\rho} | \lambda_j \rangle = p_j$. If $\hat{\rho}$ is only required to be Hermitian, then the general solution is in fact given by

$$\hat{\rho} = \rho_r + \sum_{j \neq k=0}^{r-1} |\lambda_j\rangle c_{jk} \langle \lambda_k| + W, \quad (\text{A2})$$

where W is a traceless Hermitian operator outside the support of ρ ($W\rho = 0 = \rho W$). Moreover, $p_{j \geq r} = 0 = \langle \lambda_{j \geq r} | \hat{\rho} | \lambda_{j \geq r} \rangle$ implies that W is represented by a hollow (all diagonal entries equal to zero) Hermitian matrix in the basis $\{|\lambda_{j \geq r}\rangle\}$ with arbitrary off-diagonal entries. The Hermitian solution subspace for $\hat{\rho}$ has thus a nonzero volume under some metric.

It is now obvious that if one chooses $|\phi\rangle$ to be the eigenket of W that gives a negative eigenvalue, one expects $\langle \phi | \hat{\rho} | \phi \rangle = \langle \phi | W | \phi \rangle < 0$. This implies that any such nonzero traceless W always results in a nonpositive $\hat{\rho}$. If the quantum positivity constraint is imposed on the solution for the Born probabilities, we must necessarily have $W = 0$.

This leaves the operator $A = \sum_{j \neq k=0}^{r-1} |\lambda_j\rangle c_{jk} \langle \lambda_k|$ in the right-hand side of Eq. (A2). For pure states ($r = 1$), A is clearly zero, so that $\hat{\rho} = \rho_1 = |\lambda_1\rangle \langle \lambda_1|$ is the unique positive estimator after measuring ρ_1 as we expect. For $1 < r \leq d$, we note that if $\hat{\rho}$ is to be consistent with probabilities $\langle w_j | \hat{\rho} | w_j \rangle = \langle w_j | \rho_r | w_j \rangle$ obtained from any other orthonormal measurement basis $\{|w_j\rangle\}$, then $\langle w_j | A | w_j \rangle = 0$ for all $1 \leq j \leq d-1$. As A has exactly $r^2 - r$ free parameters, it follows that measuring $k_0 = \lceil (r^2 - r)/(d-1) \rceil + 1$ linearly independent bases results in the unique solution $A = 0$ to $k_0(d-1)$ (pseudo-)invertible linear equations. When $r^2 - r \leq d-1$, measuring just one basis other than the eigenbasis will result in a unique $\hat{\rho}$. If $r = d$, we then obtain the familiar minimal bases number $k_0 = d + 1$.

To summarize, the quantum positivity constraint restricts the possible solution set consistent with probabilities derived from any given rank- r state ρ_r to a unique state estimator if the eigenbasis of ρ_r and $\lceil (r^2 - r)/(d-1) \rceil$ other orthonormal bases are measured. The method of ACT strives to achieve a small number k_{IC} of optimal IC bases that is bounded from below by k_0 . Looking at two extremal cases, measuring \mathcal{B}_{ρ_r} immediately gives us the unique estimator for any pure state, whereas the minimal number of bases needed to characterize a full-rank state is certainly $k_0 = d + 1$.

Appendix B: The size monotone

The *size monotone* $0 \leq s_{\text{CVX},k} \leq 1$ for the data convex set \mathcal{C}_k is a (non-strict) monotonically increasing function with its

size $s_k (s_{\text{CVX},k} > s_{\text{CVX},k+1} \implies s_k > s_{k+1})$.

To define a size monotone for any data convex set \mathcal{C}_k , we first pre-choose a concave function $f(\rho)$ of a unique maximum to characterize \mathcal{C}_k . In the absence of statistical fluctuation, we have the set inequality chain $\mathcal{C}_1 \supseteq \mathcal{C}_2 \supseteq \dots \supseteq \mathcal{C}_{d+1}$ as linear independent bases are sequentially measured: states in the data convex set are ruled out as more information is gained through measurements. By the concavity of $f(\rho)$ we have $f_{\text{max},1} \geq f_{\text{max},2} \geq \dots \geq f_{\text{max},d+1}$ and $f_{\text{min},1} \leq f_{\text{min},2} \leq \dots \leq f_{\text{min},d+1}$. It is clear that if $f_{\text{max},k+1} - f_{\text{min},k+1} < f_{\text{max},k} - f_{\text{min},k}$, then $\mathcal{C}_{k+1} \subset \mathcal{C}_k$ or $s_{k+1} < s_k$.

It follows immediately that if $s_{\text{CVX},k} \equiv (f_{\text{max},k} - f_{\text{min},k}) / (f_{\text{max},1} - f_{\text{min},1})$, then $s_{\text{CVX},k}$ is a size monotone that decreases with increasing k . When $s_{\text{CVX},k=k_{\text{IC}}} = 0$, the convexity of $\mathcal{C}_{k_{\text{IC}}}$ implies that $s_{k_{\text{IC}}} = 0$ as $\mathcal{C}_{k_{\text{IC}}}$ must contain only ρ_r due to the unique maximum possessed by f . Similar arguments hold for a convex f . Since $f_Z(\rho)$ is a positive linear function it can also be used to formulate the size monotone as it facilitates the class of semidefinite programs known to give a unique maximum as well as minimum in the quantum state space.

It is easy to see that $s_{\text{CVX},k_{\text{IC}}} = 0$ still implies that $s_{k_{\text{IC}}} = 0$ with noisy data that may come from statistical fluctuation or other systematic errors. For this, we can define \mathcal{C}_k to be the set of states that maximizes the likelihood function, of the exemplifying multinomial form $L(n_{j'k'} | \rho') = \prod_{k'=1}^k \prod_{j'=0}^{d-1} p_{j'k'}^{n_{j'k'}}$ for typical physical problems involving independent single-copy sampling up to a fixed total sample size $\sum_{k'=1}^k \sum_{j'=0}^{d-1} n_{j'k'} = N$ derived from the observed frequencies $n_{j'k'}$ labeled by the outcome j' and basis k' numbers. It is clear that if the data are noiseless, the maximum of L gives precisely $\hat{\rho}_{\text{ML}} = \rho_r$, so such a definition is a valid generalization to real experimental scenarios. It is important to note that while the set inequality chain “ $\mathcal{C}_{k+1} \subset \mathcal{C}_k$ ” is in general broken, that is $s_{\text{CVX},k}$ no longer behaves as a size monotone in k , the newly defined \mathcal{C}_k s are still convex sets because $\log L(n_{j'k'} | \rho')$ is a concave function and hence possesses a convex plateau structure for non-IC data. The convexity of \mathcal{C}_k arises more generally from any kind of concave $\log L(n_{j'k'} | \rho')$, which behavior is common in experiments. This is the only crucial property to again conclude that $s_{\text{CVX},k_{\text{IC}}} = 0 \implies s_{k_{\text{IC}}} = 0$. It therefore follows that the ICC protocol introduced in the main article for ACT is perfectly robust to noisy data, in the sense that the set of measurement bases $\mathcal{B} = \{\mathcal{B}_1, \mathcal{B}_2, \dots, \mathcal{B}_{k_{\text{IC}}}\}$, along with their collected data, always give a unique state reconstruction for the value of k_{IC} decided by ICC even with noisy data. No premature termination of ACT will occur. On the other hand, the final unique state estimator, of course, will have a lower statistical accuracy because of data noise.

Appendix C: The spectral decomposition of states in \mathcal{C}

For an integer k and a noiseless scenario, the data convex set \mathcal{C}_k contains all quantum states that are consistent with the bases measurements $\mathcal{B} = \{\mathcal{B}_1, \dots, \mathcal{B}_k\}$. Suppose that $\mathcal{C}_k \neq$

$\{\widehat{\rho}_{\text{ML}}\}$ We would like to check how frequently a randomly chosen state $\rho' \in \mathcal{C}_k$ possesses an eigenbasis equal to \mathcal{B}_j for some $1 \leq j \leq k$.

It is easy to see that if $\rho' = \sum_l |\lambda_{lj}\rangle \lambda_{lj} \langle \lambda_{lj}| \in \mathcal{C}_k$ where $\mathcal{B}_j = \{|\lambda_{lj}\rangle \langle \lambda_{lj}|\}$, then we must have the eigenvalues $\lambda_{lj} = p'_{lj} = \langle \lambda_{lj} | \rho' | \lambda_{lj} \rangle$ according to the definition of \mathcal{C}_k . A trivial example occurs when $k = 1$, where \mathcal{C}_1 contains exactly one

diagonal state in the measurement basis. It follows immediately that there can exist at most k states in \mathcal{C}_k that possesses eigenbases overlapping with \mathcal{B} , which are clearly measure zero compared to the infinitely many states in \mathcal{C}_k . This implies that \mathcal{C}_k for $k < k_{\text{IC}}$ contains states with eigenbases that are distinct from \mathcal{B} as the only measurable states. We add that the actual number of states with such eigenbases is generally much lower than k since for $k > 1$, every state in \mathcal{C}_k must satisfy *all* probability constraints.

-
- [1] I. Chuang and M. Nielsen, *Quantum Computation and Quantum Information* (Cambridge University Press, Cambridge, 2000).
- [2] M. G. A. Paris and J. Řeháček, eds., *Quantum State Estimation*, Lect. Not. Phys., Vol. 649 (Springer, Berlin, 2004).
- [3] Y. S. Teo, *Introduction to Quantum-State Estimation* (World Scientific Publishing Co., Singapore, 2015).
- [4] H. Häffner, W. Hänsel, C. F. Roos, J. Benhelm, D. Chek-al kar, M. Chwalla, T. Körber, U. D. Rapol, M. Riebe, P. O. Schmidt, C. Becher, O. Gühne, Dür W., and R. Blatt, “Scalable multiparticle entanglement of trapped ions,” *Nature* **438**, 643 (2005).
- [5] J. G. Titchener, M. Gräfe, R. Heilmann, A. S. Solntsev, A. Szaimeit, and A. A. Sukhorukov, “Scalable on-chip quantum state tomography,” *NJP Quantum Inf.* **4**, 19 (2018).
- [6] D. Donoho, “Compressed sensing,” *IEEE Trans. Inf. Theory* **52**, 1289 (2006).
- [7] E. J. Candès and T. Tao, “Near-optimal signal recovery from random projections: Universal encoding strategies?” *IEEE Trans. Inf. Theory* **52**, 5406 (2006).
- [8] E. J. Candès and B. Recht, “Exact matrix completion via convex optimization,” *Found.Comput.Math.* **9**, 717 (2009).
- [9] D. Gross, Y.-K. Liu, S. T. Flammia, S. Becker, and J. Eisert, “Quantum state tomography via compressed sensing,” *Phys. Rev. Lett.* **105**, 150401 (2010).
- [10] A. Kalev, R. L. Kosut, and I. H. Deutsch, “Quantum tomography protocols with positivity are compressed sensing protocols,” *NJP Quantum Inf.* **1**, 15018 (2015).
- [11] A. Steffens, C. A. Riofro, W. McCutcheon, I. Roth, B. A. Bell, A. McMillan, M. S. Tame, J. G. Rarity, and J. Eisert, “Experimentally exploring compressed sensing quantum tomography,” *Quantum Sci. Technol.* **2**, 025005 (2017).
- [12] C. A. Riofrío, D. Gross, S. T. Flammia, T. Monz, D. Nigg, R. Blatt, and J. Eisert, “Experimental quantum compressed sensing for a seven-qubit system,” *Nat. Commun.* **8**, 15305 (2017).
- [13] C. H. Baldwin, I. H. Deutsch, and A. Kalev, “Strictly-complete measurements for bounded-rank quantum-state tomography,” *Phys. Rev. A* **93**, 052105 (2016).
- [14] W. Pauli, *Die allgemeinen Prinzipien der Wellenmechanik, Handbuch der Physik*, edited by H. Geiger and K. Scheel, Vol. 24 (Springer-Verlag, Berlin, 1933).
- [15] C. Carmeli, T. Heinosaari, J. Schultz, and A. Toigo, “How many orthonormal bases are needed to distinguish all pure quantum states?” *Eur. Phys. J. D* **69**, 179 (2015).
- [16] L. Vandenberghe and S. Boyd, “Semidefinite programming,” *SIAM Review* **38**, 49 (1996).
- [17] A. S. Bandeira, E. Dobriban, D. G. Mixon, and W. F. Sawin, “Certifying the restricted isometry property is hard,” *IEEE Trans. Inf. Theory* **59**, 3448 (2013).
- [18] J. Řeháček, Z. Hradil, E. Knill, and A. I. Lvovsky, “Diluted maximum-likelihood algorithm for quantum tomography,” *Phys. Rev. A* **75**, 042108 (2007).
- [19] J. Shang, Z. Zhang, and H. K. Ng, “Superfast maximum-likelihood reconstruction for quantum tomography,” *Phys. Rev. A* **95**, 062336 (2017).
- [20] Y. S. Teo, H. Zhu, B.-G. Englert, J. Řeháček, and Z. Hradil, “Quantum-state reconstruction by maximizing likelihood and entropy,” *Phys. Rev. Lett.* **107**, 020404 (2011).
- [21] S. Huang, D. N. Tran, and T. D. Tran, “Sparse signal recovery based on nonconvex entropy minimization,” *IEEE (ICIP 2016)*, 3867 (2016).
- [22] D. N. Tran, S. Huang, S. P. Chin, and T. D. Tran, “Low-rank matrices recovery via entropy function,” *IEEE (ICASSP 2016)*, 4064 (2016).
- [23] M. Kech and M. M. Wolf, “Constrained quantum tomography of semi-algebraic sets with applications to low-rank matrix recovery,” *Information and Inference: A Journal of the IMA* **6**, 171 (2016).
- [24] E. Bolduc, N. Bent, E. Santamato, E. Karimi, and R. W. Boyd, “Exact solution to simultaneous intensity and phase encryption with a single phase-only hologram,” *Opt. Lett.* **308**, 3546 (2013).
- [25] F. Bouchard, N. H. Valencia, F. Brandt, R. Fickler, M. Huber, and M. Malik, “Measuring azimuthal and radial modes of photons,” *Opt. Express* **26**, 31925 (2018).